

## Icosahedral aluminum—transition-metal alloys

Peter A. Bancel and Paul A. Heiney

Department of Physics, University of Pennsylvania, Philadelphia, Pennsylvania 19104-6396  
and Laboratory for Research on the Structure of Matter, University of Pennsylvania,  
Philadelphia, Pennsylvania 19104-3859

(Received 30 December 1985)

We have used x-ray and electron diffraction to study the icosahedral phase in rapidly quenched alloys of Al with Mn, Re, Cr, Ru, V, Mo, and W. We also find negative results in searches for the icosahedral phase in various other transition-metal alloys. Addition of small amounts of Si and Ru to Al-Mn and Al-Cr alloys appears to enhance stability of the icosahedral phase. We discuss the role of atomic packing, electronegativity differences, and electronic band structure in stabilizing this phase.

## INTRODUCTION

The discovery last year of an icosahedral phase (IP) in quenched alloys of Al with Mn, Cr, and Fe has presented an intriguing problem in crystallography.<sup>1</sup> Icosahedral rotational symmetry is incompatible with periodic translational order, yet the new IP's exhibit diffraction patterns with sharp spots, a property normally associated with periodic crystals. A possible resolution of these observations was suggested by Levine and Steinhardt,<sup>2</sup> who introduced a class of structures which have long-range bond-orientational order and perfect quasiperiodic translational order. The calculated diffraction patterns of these icosahedral quasicrystals were found to be in close agreement with the electron diffraction patterns of the Al-Mn IP. Quasicrystals have since been investigated from several points of view<sup>3-5</sup> and have been shown to include structures of arbitrary symmetry,<sup>6</sup> with orientational order preserved across the grain.

Landau theory calculations<sup>7-12</sup> have shown that quasiperiodic icosahedral structures may indeed be metastable, and possibly even globally stable, with respect to competing crystalline phases. It therefore seems plausible that the IP is not peculiar to Al-Mn, Al-Cr, and Al-Fe, but may be realized in many other systems, and indeed it has recently been reported in  $U_{20}Pd_{60}Si_{20}$  (Ref. 13) and  $Al_{44}Mg_{36}Zn_{15}Cu_5$  (Ref. 14) alloys. We present here the results of a survey of quenched aluminum—transition-metal (Al-*M*) alloys. The intention of this study is to determine which Al-*M* systems form the IP and to investigate what factors favor its formation. In addition to gaining insight into the structural properties, information about general alloying principles of the IP may lead to improved samples. This is important since many experiments are presently limited by sample quality. An investigation of quenched Al-Mn has been presented elsewhere.<sup>15</sup> We first review those results.

Initial studies were done on rapidly quenched 6:1 Al-Mn samples. Quenching from the melt yields a mixture of fcc-Al and the IP. Electron microscopy studies show grains of the IP ranging up to several microns in size, embedded in an aluminum matrix. Electron diffraction from

a single grain shows patterns of icosahedral symmetry. The presence of excess Al implies that the concentration of Mn in the IP is greater than 1:6, and measurements on other samples have put the Mn content of the IP at 21.5–22 at. %. Stoichiometric samples show no excess Al. However, as the Mn content is increased towards stoichiometry, competition from another metastable Al-Mn (Ref. 16) phase develops. This “*T* phase” forms at slightly slower quenching rates than the IP and can be suppressed by appropriate adjustment of quenching parameters. Although the *T* phase in itself merits further study, it poses problems for any measurements of bulk IP samples, since the *T* phase and IP structures appear to be closely related. In particular, quantitative powder-diffraction measurements of the IP may be unreliable if samples contain more than several percent *T* phase, since many diffraction peaks of the two phases overlap.

As previously discussed,<sup>15</sup> the electron-diffraction patterns can be indexed by a set of basis vectors taken as the vertex vectors of an icosahedron. Determining the  $|q|$  values from electron diffraction allows the indexing of x-ray power-diffraction profiles, which can then be used for preliminary identification of the IP in new alloys. The widths of peaks in high-resolution x-ray scans range from  $0.04 \text{ \AA}^{-1}$  to  $0.01 \text{ \AA}^{-1}$ , corresponding to translational correlation lengths on the order of 100 Å. This should be compared with the extent of orientational order (grain sizes of several microns). It remains to be seen if the broad peak widths are due to symmetry-dependent strains, defects, or other mechanisms. X-ray powder scans, which can reveal the presence of contaminant phases in bulk samples, also show considerable diffuse scattering around the most intense peaks. This may indicate disorder in the icosahedral quasilattice or perhaps small amounts of glassy Al-Mn present in the samples.

## EXPERIMENTAL DETAILS

Our present study investigates phase formation in 14 Al-*M* alloys. Thin-ribbon samples of these alloys were prepared by conventional melt-spinning techniques. In order to ascertain the relative tendency for IP formation

in these systems, the spinning parameters were held fixed and chosen so that a stoichiometric Al-Mn alloy (21.5–22 at. % Mn) would quench to nearly single-phase icosahedral ribbons. X-ray scans from a number of such Al-Mn samples show identical diffraction profiles, indicating that the procedure is reproducible. Alloys were prepared by induction-melting high-purity (better than 99.95%, in most cases) elemental constituents in an argon environment. The spinning apparatus consisted of a quartz nozzle suspended above a 23-cm Cu wheel rotating at 3600 revolutions per minute. Alloys were induction melted in the nozzle in gently flowing argon, then propelled through a 0.4-mm aperture at the tip of the nozzle onto the wheel by a pressure burst of 40 lbs. per square inch. This produced brittle ribbons several millimeters wide and 20–40 microns thick. The quench rate could be increased by increasing either the rotation speed of the wheel or the pressure above the molten alloy, with similar results. Our experience with Al-Mn has indicated that near stoichiometry other phases may compete with the IP. For this reason, samples for a number of systems were made at several Al-rich compositions.

Samples were characterized with electron diffraction and powder x-ray diffraction. The x-ray measurements employed Mo  $K\alpha$  radiation from a Rigaku RU-200 rotating-anode generator, operating at 9 kW. The x rays were monochromatized by Bragg reflection from a 2-in. bent graphite crystal and further collimated by slits before and after the sample, resulting in an instrumental resolution of  $0.012 \text{ \AA}^{-1}$  half width at half maximum (HWHM). Note that in most cases observation of weak peaks was limited, not by lack of x-ray intensity, but rather by intrinsic diffuse scattering from the sample. Samples for

x-ray study were gently ground into a powder and suspended between pieces of Kapton tape. (It was found that grinding the sample too violently could result in substantial degradation of the x-ray spectra, presumably because of microscopic morphological changes.) Diffraction scans for each sample were indexed to known equilibrium crystalline structures or the IP. In only two cases did there occur peaks that could not be indexed. Every occurrence of the IP was confirmed by single-grain diffraction in a Phillips 400T electron microscope. We emphasize that the survey determines the relative tendencies for formation of the IP in these systems. Since the x-ray scans cannot detect the presence of less than a few percent of the IP in a sample, a null result indicates only that its formation is unfavorable. A case in point is Al-Fe which shows no sign of icosahedral peaks in x-ray scans, yet is known to form the IP.<sup>1</sup>

#### Al-TRANSITION-METAL BINARY COMPOUNDS

We have identified the IP in seven of the Al- $M$  systems surveyed ( $M = \text{Mn, Re, Cr, Ru, V, W, Mo}$ ). We searched for, but did not find, evidence of the IP in binary alloys of Al with Ti, Fe, Co, Rh, Pd, Ta, and Pt. (Al-Pd and Al-Pt easily formed  $T$  phase, however.) In order to make comparisons between systems containing the IP, it is helpful to consider three different factors: (1) the degree of positional order as measured by the width of the sharpest diffraction peak, which is the  $I(100000)$  in our indexing scheme, occurring at around  $2.9 \text{ \AA}^{-1}$ , (2) the extent of orientational order as indicated by grain size, and (3) the relative phase stability as indicated by presence or absence of other phases. We can use these factors to make a qual-

TABLE I. Phases found in rapidly quenched alloys of Al with various transition-metal ( $M$ ) atoms at approximately 4:1, 6:1, and 12:1 compositions. Abbreviations are the following: IP (icosahedral phase), TP ( $T$  phase), Al (crystalline fcc-Al), and ? (unknown phases). Only phases found in quantities greater than a few percent are shown. The fourth column shows the approximate size ratios of Al and  $M$  atoms (Refs. 25 and 26). For ideal icosahedral packing of spheres, this ratio would be 0.905. For samples displaying the IP, columns 6 through 8 display the largest grain sizes (in microns) typically found by electron microscopy, the approximate HWHM of the sharp (100000) x-ray peak (in  $\text{\AA}^{-1}$ ), and the percent expansion of the lattice relative to Al-Mn as derived from the shift in x-ray peak positions. Alloys which do not show the IP are listed in the bottom half of the table.

$M$	4:1	6:1	12:1	Size ratio	Grain size ( $\mu\text{m}$ )	HWHM ( $\text{\AA}^{-1}$ )	Expansion (%)
Mn	IP	IP + Al		0.90	1-2	0.009	$\equiv 0.0$
Re	IP	IP + Al		0.96	1-2	0.02	+ 1.2
Cr	IP + ?	IP + Al		0.92	1-2	0.015	+ 1.1
Ru	IP + Al + $\text{Al}_{13}\text{Ru}_4$			0.94	1	0.02	- 1.1
V	$\text{Al}_3\text{V} + \text{Al}$	IP + Al		0.94	< 1	0.03	+ 3.0
W		IP + Al	IP + Al	0.98	0.1	0.06	+ 3.0
Mo	$\text{Al}_3\text{Mo} + ?$	$\text{Al}_3\text{Mo} + \text{Al} + ?$	IP + Al	0.97	0.1	0.06	+ 3.0
Pd	TP	TP + Al		0.96			
Pt	TP	TP + Al		0.97			
Ti	$\text{AlTi} + \text{Al}$			1.03			
Fe	$\text{Al}_{13}\text{Fe}_4 + \text{Al}$	$\text{Al}_{13}\text{Fe}_4 + \text{Al}$	$\text{Al}_{13}\text{Fe}_4 + \text{Al}$	0.89			
Co	$\text{Al}_9\text{Co}$			0.89			
Rh	$\text{Al}_9\text{Rh}_2$	$\text{Al}_9\text{Rh}_2 + \text{Al}$		0.94			
Ta	$\text{Al}_3\text{Ta} + \text{Al}$		$\text{Al}_3\text{Ta} + \text{Al}$	1.03			

itative ranking of the different icosahedral systems (see Table I). A representative set of diffraction scans is shown in Fig. 1. As a reference, Fig. 1(a) shows a diffraction profile from a stoichiometric (78.4 at. % Al) Al-Mn sample which has been stabilized by the addition of a small amount of Ru, as discussed below. The IP can be recognized easily by the three pairs of strong peaks at approximately 1.7, 3.0, and 4.25  $\text{\AA}^{-1}$  and is indexed as shown. Note the use of a logarithmic intensity scale; plotting the data in this way emphasizes weak peaks and diffuse scattering at the expense of exaggerating noise and distorting peak shapes.

A typical scan from an Al-Mn binary alloy [Fig. 1(b)] has a similar diffraction profile but contains several low-

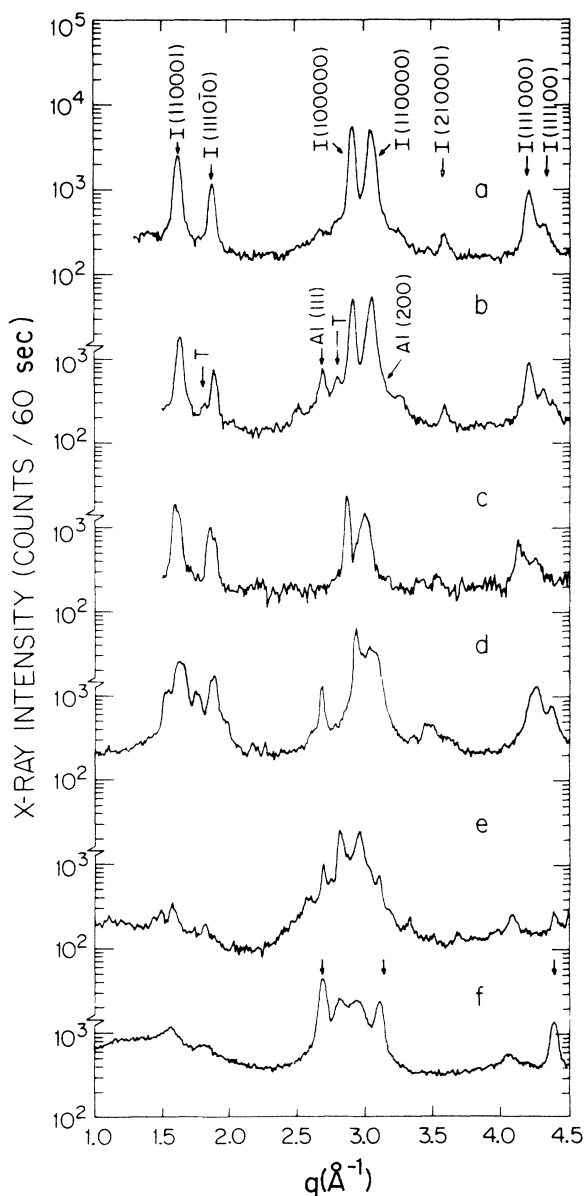


FIG. 1. X-ray powder-diffraction profiles from rapidly quenched Al-M alloys. Note logarithmic scale. (a)  $\text{Al}_{78.4}\text{Mn}_{17.6}\text{Ru}_4$ ; (b)  $\text{Al}_{80.4}\text{Mn}_{19.6}$ ; (c)  $\text{Al}_{78}\text{Re}_{22}$ ; (d)  $\text{Al}_{79}\text{Ru}_{21}$ ; (e)  $\text{Al}_{85.7}\text{V}_{14.3}$ ; (f)  $\text{Al}_{92.3}\text{Mo}_{7.7}$ .

intensity peaks which cannot be icosahedrally indexed, and indicate the presence of contaminant phases. The sample composition is slightly Al rich (80.4% Al) so that the excess fcc-Al has precipitated between IP grains, giving rise to the Al(111) reflection at 2.69  $\text{\AA}^{-1}$ , as indicated. Two other peaks at 2.80 and 1.81  $\text{\AA}^{-1}$  signal the presence of *T* phase, as does a slight broadening of the *I*(110000) which is nearly coincident with a third strong *T*-phase peak. As mentioned above, it is this overlapping of numerous peaks between these two phases that hinders quantitative analysis of the scattering data. A scan from a stoichiometric Al-Re sample is shown in Fig. 1(c). The sample is nearly single phase and peak widths are slightly broader than those seen in Al-Mn scans. A comparison with Fig. 1(b) shows that relative peak intensities are somewhat altered, a consequence of increased scattering from the heavy Re atoms. The Al-Mn and Al-Re systems are the best of the Al-M IP's that we have found.

The remaining five icosahedral Al-M binary alloys are of much poorer quality. An x-ray scan of an  $\text{Al}_{79}\text{Ru}_{21}$  alloy is shown in Fig. 1(d). The system is three phase and indexes to the IP, fcc-Al, and crystalline  $\text{Al}_{13}\text{Ru}_4$ . If the quenching rate is increased by increasing the wheel velocity, the amount of Al and of  $\text{Al}_{13}\text{Ru}_4$  decrease, implying that single-phase icosahedral Al-Ru might be formed at yet higher quenching rates. Both grain sizes and translational correlation lengths are noticeably smaller in these samples than in Al-Mn, and these do not improve at higher quenching rates. A stoichiometric Al-V alloy spun at our standard quenching rate produced a two-phase system of  $\text{Al}_3\text{V}$  and fcc-Al. The IP could only be formed at an Al-rich composition of  $\geq 85\%$  Al. X-ray scans [Fig. 1(e)] show peaks from the two phases and a broad diffuse scattering intensity around 2.9  $\text{\AA}^{-1}$ . As mentioned earlier, this diffuse scattering occurs in all systems, but it is most pronounced in those of poorer quality. Finally, Fig. 1(f) shows a diffraction scan of  $\text{Al}_{92.3}\text{Mo}_{7.7}$ . Samples at 4:1 and 6:1 Al-Mo compositions both produced crystalline phases. The IP appears in this 12:1 sample, but clearly the icosahedral ordering is very poor. The peaks are broad and there is a large amount of diffuse scattering. Microscopy showed the grain sizes to be 1000  $\text{\AA}$  or less. The Al-W system has similar characteristics.

The seven icosahedral binary alloys are formed with transition metals which are grouped in the center of the periodic chart. Not surprisingly, they have similar phase diagrams with Al and share several isomorphous structures. These results suggest that Al-Tc and Al-Os would quench to the IP as well.

#### TERNARY AND QUATERNARY COMPOUNDS

It has been noted<sup>17</sup> that the icosahedral ordering in Al-Mn is improved by the replacement of a few percent Al with Si in the sample composition. Diffraction intensities are altered slightly so that weak reflections, unseen in binary samples, become visible in electron-diffraction pictures and micrographs of single grains show significantly reduced strains. Evidence for increased icosahedral order is also seen in the x-ray data. Peak widths sharpen by up to 50%, indicating a larger positional correlation length,

and the presence of  $T$  phase is reduced. An x-ray scan of  $\text{Al}_{74.5}\text{Mn}_{21}\text{Si}_{4.5}$  [Fig. 2(a)] reveals almost no  $T$  phase, with only the most intense reflection of  $2.8 \text{ \AA}^{-1}$  appearing above the background scattering. However, the addition of Si has induced the growth of another phase, which becomes more prevalent with increasing Si content. An  $\text{Al}_{71.5}\text{Mn}_{21}\text{Si}_{7.5}$  sample [Fig. 2(b)] shows more clearly a number of peaks from this phase which we identify as crystalline  $\beta(\text{Al-Mn-Si})$ .<sup>18</sup> At our standard quenching rate, the Si content which minimizes the  $T$  and  $\beta(\text{Al-Mn-Si})$  phases is around 4%. At higher quenching rates the  $\beta$  phase is suppressed so that single-phase samples are not restricted to such low Si concentrations. The effects of Si additions appears to be limited to the Al-Mn system. Inclusions of 4% Si in alloys of Al with V, Cr, Fe, Ru, Pd, and Re produced no significant changes in the diffraction profiles.

It is reasonable to consider a similar substitution for the transition-metal constituent, particularly in light of recent Mössbauer (Ref. 19) and EXAFS (Ref. 20) measurements which suggest the presence of at least two Mn sites in icosahedral Al-Mn. We have investigated this question by replacing Mn with 2–11 at. % Ru and have found that the Ru addition greatly increases the IP stability relative to that of the  $T$  phase. Figures 2(c) and 2(d) compare the x-ray scans of Al-Mn and Al-Mn-Ru samples which have been spun at low quenching rates. The Al-Mn scan reveals large amounts of fcc-Al and  $T$  phase whereas the Al-Mn-Ru is single phase. The  $T$  phase suppression has been found to be strong in samples with 4 and 6% Ru. At a composition of 11 at. % Ru,  $\text{Al}_{13}\text{Ru}_4$  forms as a contaminant phase. The increased stability of the IP has been gained at the expense of positional order, as can be seen by the noticeably broader peak widths. This is not so for the Al-Cr system [Fig. 2(e)] for which the addition of Ru also suppressed a contaminant phase (not identified). The x-ray scans show that the width of the sharp (100000) peak actually decreases to  $0.005 \text{ \AA}^{-1}$ , indicating an increased positional correlation length. Likewise, grain sizes measured from electron micrographs extend up to  $25 \mu\text{m}$ . Electron diffraction pictures from Al-Cr-Ru show an increased number of weak spots as in the case of Al-Mn-Si, and it has been possible to identify and index nearly 200 independent reflections. We have also observed up to 45 icosahedral x-ray powder pattern peaks in these samples. Finally, the addition of a few percent Si [Fig. 2(f)] to the Al-Mn-Ru samples sharpens the diffraction peaks without introducing any new additional phases.

We have also studied the effects of Ru additions to Al-V, Al-Fe, and Al-Pd and have found no noticeable difference in the tendency of these alloys to form the IP. Nevertheless, considering the significant effects observed in the Al-Mn-Ru and Al-Cr-Ru systems, it is plausible to suggest that the two transition metals are occupying different sites, and that these sites are chemically as well as crystallographically distinguishable.

#### DISCUSSION: STABILITY OF THE ICOSAHERAL PHASE

An alloy structure will be stable if its free energy  $F = U - TS$  exhibits a minimum. For most solid phases,

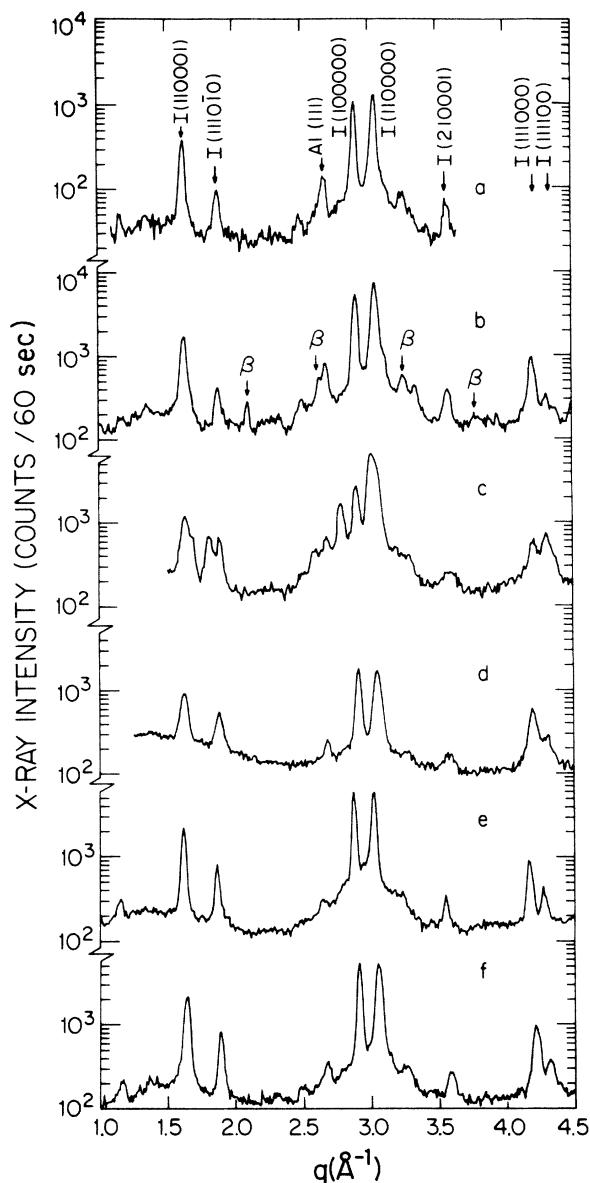


FIG. 2. X-ray diffraction profiles of ternary and quaternary compounds. (a)  $\text{Al}_{74.5}\text{Mn}_{21}\text{Si}_{4.5}$ ; (b)  $\text{Al}_{71.5}\text{Mn}_{21}\text{Si}_{7.5}$  [arrows indicate positions of  $\beta(\text{Al-Mn-Si})$  peaks]; (c)  $\text{Al}_{80}\text{Mn}_{20}$  (slow quench); (d)  $\text{Al}_{79}\text{Mn}_{17}\text{Ru}_4$  (slow quench); (e)  $\text{Al}_{79}\text{Cr}_{17}\text{Ru}_4$ ; (f)  $\text{Al}_{75.5}\text{Mn}_{17.5}\text{Ru}_4\text{Si}_3$ .

at constant values of pressure and temperature, this reduces to a minimization of the internal energy  $U$ . Much of the theory of alloy phases is concerned with understanding which factors strongly influence the internal energy and why. Among the most prominent factors are electronegativity differences, atomic size ratios, and band-structure considerations. The first two of these are largely involved with local structure and ordering. Energy-band considerations must include the effects of more distant atoms, especially in metals, where conduction electrons are delocalized throughout the structure.

The icosahedral Al-*M* binary alloys are metastable and therefore occupy a local minimum in free-energy space. It is tempting to offer an explanation of this minimum in terms of the energy factors listed above.

The least important of these factors is the electronegativity difference  $\Delta\chi$ . When large electronegativity differences exist between atoms, the effects on alloy-phase stability are demonstrable, but when differences are about 0.5 units or less, electronegativities generally cease to play a role. The electronegativity of Al is<sup>21</sup> 1.5 and the range of  $\Delta\chi$  over all Al-*M* binary alloys is +0.3 to -0.7. The value of  $\Delta\chi$  for Al-Mn is zero.

The ratio of atomic sizes influences the packing of atoms and the possibilities for local coordination. It is evident that the IP contains at least two different sizes of atom, and since the ratio of the sizes of Mn to Al is very nearly that required for perfect packing of hard spheres in icosahedral coordination polyhedra, models based on the packing of Al-Mn icosahedra have been proposed.<sup>22-24</sup> Table I shows the size ratios<sup>25,26</sup> for the Al-*M* binary alloys we have studied. Among the icosahedral binary alloys, the largest *M* atoms (Mo and W) form the poorest IP's, but beyond that there is no apparent trend. However, the sizes of atoms in metals vary according to the electronic structure and can be difficult to define in complex structures if there is more than one near-neighbor distance for a given site. Table I also lists the expansion of the icosahedral lattices, relative to Al-Mn, as derived from the absolute positions of diffraction peaks. Assuming that the size of Al atoms does not vary, this can be taken as an indication of the relative transition-metal sizes in the IP, when appropriately scaled by the stoichiometry. The binary alloys with lattice parameters closest to that of Al-Mn form the better IP's as one would expect, but the lack of correlation with elemental atomic sizes suggests that bonding and electronic factors play a strong role in determining interatomic distances. Compare, for instance, the differences between the V and Re IP's. It is interesting to note that the Ru system is contracted relative to Al-Mn even though elemental Ru is about 3% larger than Mn, a situation which may be due in part to the Al-Ru  $\Delta\chi$  of 0.7.

We now discuss the role of energy-band factors in determining the formation of IP's. It was recognized by Hume-Rothery<sup>27</sup> that simple alloys based on the noble metals assume stable structures at fixed values of electron concentration, defined as the number of conduction electrons per atom. Jones<sup>28</sup> interpreted this observation in terms of a rigid-band model in which valence electrons of constituent atoms were placed in a common band. The presence of a Brillouin-zone boundary opens gaps in the free-electron dispersion relation,  $E(k)$ , producing kinks in the density of states and lowering the total energy of the free-electron gas. Jones showed that this mechanism could account for the Hume-Rothery rules. At a given electron concentration the total energy is lowered if the system assumes a structure which places a zone boundary in contact with the Fermi surface. Even in a disordered alloy, if intense diffraction peaks are associated with large band gaps,<sup>28</sup> a pseudo-Brillouin-zone can be constructed by planes perpendicular to the corresponding reciprocal-

lattice vectors. The volume of the zone,  $V$ , together with the mean atomic volume  $v$ , determine the number of electrons per atom most favorable for the structure, which can be shown to be  $2Vv$ . This rule has been applied in the analysis of numerous types of structure including superlattice formation and stacking faults,<sup>29</sup> and more recently, metallic glasses.<sup>30</sup>

The presence of transition metals complicates this type of analysis since it is not clear how many electrons are donated by the *d* bands to the conduction band of the alloy. The usual approach is to assume a transfer of charge from the conduction band into the *d* bands in order to compensate for the unpaired spins of the transition metal. The transition metal is accordingly assigned a negative valence. This hypothesis is consistent with the observations that the Mn atom is nonmagnetic in Al-rich Al-Mn alloys. Investigations of charge transfer in Al-*M* alloys generally show substantial charge transfer, although the magnitude of the transfer is uncertain. For example, a simple analysis which compensates the unpaired spins in elemental Mn would assign<sup>31</sup> a valency of -3.66, whereas measurements of Al-rich Al-Mn alloys assign<sup>32,33</sup> valencies ranging from -2 to -3.6. Note that a precise valency determination is not required to decide whether IP formation is consistent with the Hume-Rothery mechanism, since the electron gas will have its energy lowered so long as the Fermi sphere makes appreciable contact with the pseudo-Brillouin-zone. Changes of several percent in the magnitude of the Fermi wave vector will not dramatically alter this situation. In the case of the IP, where the transition-metal (*M*) content is only 22 at.%, a 1% change in  $k_F$  corresponds to a 10% change in the *M* valency. The analysis need therefore only consider approximate values of the *M* valencies.

From this point of view, a Hume-Rothery analysis appears to work quite well for Al-*M* IP's. Although a true quasiperiodic structure is expected to have a dense set of peaks in reciprocal space, in fact we observe that strong diffraction peaks are relatively sparse. Strong x-ray diffraction peaks are found in three regions: the (110001) and (1110 $\bar{1}$ 0) near  $1.7 \text{ \AA}^{-1}$ , the (100000) and (110000) near  $3.0 \text{ \AA}^{-1}$ , and the (111000) and (111100) near  $4.25 \text{ \AA}^{-1}$ . The high multiplicity of the icosahedral peaks makes the corresponding pseudo-Brillouin-zone nearly spherical, which could result in a large overlap with the Fermi surface. A Fermi wave vector at  $k_F \approx 3.00/2 \text{ \AA}^{-1}$  implies an electron density of  $n_e = k_F^3/3(\pi^2) = 0.114e^-/\text{\AA}^3$ . From the contraction of elemental atomic volumes in Al<sub>6</sub>Mn, we estimate<sup>34-36</sup> the average atomic volume at  $15.28 \text{ \AA}^3$ , implying a valence electron concentration of 1.74 electrons per atom. Combining the optimal stoichiometry of Al<sub>78</sub>Mn<sub>22</sub> with the known Al valence of 3, we conclude that the Fermi level will overlap with the zone boundary if roughly  $[(78)3 - 174]/22 = 2.73$  electrons per Mn atom are absorbed in the *d* bands. In fact, this is in the middle of the range of measured<sup>33</sup> electron absorption values of Mn in Al<sub>6</sub>Mn. Thus it is plausible that the structure is stabilized by the presence of a large gap close to the Fermi energy. Cr compounds have been measured to have similar charge transfer, and Al-Cr IP shows peaks in nearly the same positions as those in

icosahedral Al-Mn.

By contrast, we have found that Al-Co does not form the IP. This is consistent with charge transfer measurements on Al-Co alloys<sup>33</sup> which show  $\Delta e \approx 1.6$ – $2.0$  electrons. These values are consistent with phase stabilization of the known equilibrium phase  $\text{Al}_9\text{Co}_2$ , which forms when we rapidly quench Al-Co. Note that crystalline Al-Mn and Al-Cr compounds also have strong peaks in the neighborhood of  $3 \text{ \AA}^{-1}$ . Thus it appears that the principal result of energy-band effects is to discriminate against structures which do *not* result in a band gap near the Fermi energy.

We also get good agreement with the Hume-Rothery rules using the reported  $q$  values for intense peaks in the IP of  $\text{Al}_{44}\text{Mg}_{36}\text{Zn}_{15}\text{Cu}_5$ :<sup>14</sup> the pairs of peaks equivalent to those in icosahedral Al-Mn fall near<sup>14</sup>  $1.3$ ,  $2.3$ , and  $3.3 \text{ \AA}^{-1}$ . Assuming that the density of icosahedral  $\text{Al}_{44}\text{Mg}_{36}\text{Zn}_{15}\text{Cu}_5$  is close to that of its equilibrium Frank-Kasper phases, we estimate, using the zone boundary at  $3.3 \text{ \AA}^{-1}$ , that  $e/a$  should be around  $2.6$ . Valences of the constituents (which are not complicated by half-empty  $d$  bands) imply  $e/a \approx 2.4$ , in reasonable agreement with our calculated value. Note that in this case it is the

higher-order (111000) and (111100) peaks which appear to stabilize the electronic structure.

### CONCLUSIONS

We have presented the first observations of the icosahedral phase in a number of aluminum-transition-element alloys. The addition of small amounts of Ru and Si appears to stabilize the IP, resulting in both increased translational correlation lengths and suppression of competing phases. While size ratio effects do not appear to play as obvious a role in the formation of the IP as originally suggested, simple calculations indicate that gaps in the electron band structure created by pseudo-Brillouin-zones may play a role in stabilizing the IP.

### ACKNOWLEDGMENTS

We would like to thank P. Chaikin, T. Egami, A. I. Goldman, D. Kofalt, D. Levine, P. J. Steinhardt, and P. W. Stephens for many useful discussions. This work was supported by the National Science Foundation Materials Research Laboratory Program under contract No. DMR-82-16718.

- 
- <sup>1</sup>D. Shechtman, I. A. Blech, D. Gratias, and J. W. Cahn, *Phys. Rev. Lett.* **53**, 1951 (1984).
- <sup>2</sup>D. Levine and P. J. Steinhardt, *Phys. Rev. Lett.* **53**, 2477 (1984).
- <sup>3</sup>P. Kramer, *Z. Naturforsch.* **40A**, 755 (1985).
- <sup>4</sup>V. Elser, *Acta Crystallogr. A* **42**, 36 (1986).
- <sup>5</sup>M. Duneau and A. Katz, *Phys. Rev. Lett.* **54**, 2688 (1985).
- <sup>6</sup>J. E. S. Socolar, P. J. Steinhardt, and D. Levine, *Phys. Rev. B* **32**, 5547 (1985).
- <sup>7</sup>D. Levine, T. C. Lubensky, S. Ostlund, S. Ramaswamy, and P. J. Steinhardt, *Phys. Rev. Lett.* **54**, 1520 (1985).
- <sup>8</sup>P. A. Kalugin, A. Kitaev, and L. Levitov, *J. Phys. Lett.* **46**, L-601 (1985).
- <sup>9</sup>P. Bak, *Phys. Rev. Lett.* **54**, 1517 (1985).
- <sup>10</sup>N. D. Mermin and S. Troian, *Phys. Rev. Lett.* **54**, 1524 (1985).
- <sup>11</sup>D. R. Nelson and S. Sachdev, *Phys. Rev. B* **32**, 689 (1985).
- <sup>12</sup>M. V. Jarić, *Phys. Rev. Lett.* **55**, 607 (1985).
- <sup>13</sup>S. J. Poon, A. J. Drehman, and K. R. Lawless, *Phys. Rev. Lett.* **55**, 2324 (1985).
- <sup>14</sup>N. K. Mukhopadhyay, G. N. Subanna, S. Ranganathan, and K. Chattopadhyay (unpublished).
- <sup>15</sup>P. A. Bancel, P. A. Heiney, P. W. Stephens, A. I. Goldman, and P. M. Horn, *Phys. Rev. Lett.* **54**, 2422 (1985).
- <sup>16</sup>L. Bendersky, *Phys. Rev. Lett.* **55**, 1461 (1985).
- <sup>17</sup>L. A. Bendersky and M. J. Kaufman, *Philos. Mag.* (to be published).
- <sup>18</sup>K. Robinson, *Acta Crystallogr.* **5**, 397 (1952).
- <sup>19</sup>M. Eibschutz (private communication).
- <sup>20</sup>E. A. Stern, Y. Ma, and C. E. Bouldin, *Phys. Rev. Lett.* **55**, 2172 (1985).
- <sup>21</sup>Linus Pauling, *The Nature of The Chemical Bond*, 3rd ed. (Cornell University Press, Ithaca, New York, 1960), p. 93.
- <sup>22</sup>D. Shechtman and I. A. Blech, *Metall. Trans.* **16A**, 1005 (1985).
- <sup>23</sup>K. Hiraga, M. Hirabayashi, A. Inoue, and T. Masumoto, *Sci. Rep. Res. Inst. Tohoku Univ., Ser. A* **32**, 309 (1985).
- <sup>24</sup>P. W. Stephens and A. I. Goldman, *Phys. Rev. Lett.* **56**, 1168 (1986).
- <sup>25</sup>See, for example, W. B. Pearson, *The Crystal Chemistry and Physics of Metals and Alloys* (Wiley, New York, 1972), p. 150.
- <sup>26</sup>T. Egami and Y. Waseda, *J. Non.-Cryst. Solids* **64**, 113 (1984).
- <sup>27</sup>W. Hume-Rothery, *J. Inst. Met.* **35**, 295 (1926).
- <sup>28</sup>H. Jones, *Proc. Phys. Soc. London* **49**, 250 (1937).
- <sup>29</sup>W. B. Pearson, *The Crystal Chemistry and Physics of Metals and Alloys*, (Wiley, New York, 1972), Chap. 3.
- <sup>30</sup>P. Haussler, *Z. Phys. B* **53**, 15 (1983).
- <sup>31</sup>G. E. Raynor and D. M. B. Waldron, *Philos. Mag.* **40**, 198 (1949).
- <sup>32</sup>A. Wenzel and S. Steinemann, *Helv. Phys. Acta.* **47**, 321 (1974) and references therein.
- <sup>33</sup>A. D. I. Nicol, *Acta Crystallogr.* **6**, 285 (1953).
- <sup>34</sup>We estimate a density of  $3.60 \pm 0.05 \text{ g/cm}^3$  for the Al-Mn IP. This implies a density of  $3.28 \text{ g/cm}^3$  for a sample with a 6:1 composition, in agreement with results in Refs. 35 and 36.
- <sup>35</sup>K. F. Kelton and T. W. Wu, *Appl. Phys. Lett.* **46**, 1059 (1985).
- <sup>36</sup>H. S. Chen, C. H. Chen, A. Inoue, and J. T. Krause, *Phys. Rev. B* **32**, 1940 (1985).